

## A mmWaves Channel Sounding Technique to Capture Human-induced Dynamic Multipaths

Roberto Alesii\*(1)(2), Dajana Cassioli (1), and Andreas F. Molisch(3)

- (1) Dept. of Information Engineering, Computer Science and Mathematics, University of L'Aquila, L'Aquila, 67100 Italy (2) DEWS Center of Excellence, University of L'Aquila, L'Aquila, 67100 Italy
  - (3) Dept. of Electrical and Computer Engineering, University of Southern California, Los Angeles, CA, USA {roberto.alesii, dajana.cassioli}@univaq.it, molisch@usc.edu

#### Abstract

Design and standardization of future millimeter-wave (mmWave) wireless communications systems require accurate models of wireless propagation channels. In particular, comprehensive statistical models describing the effect of human bodies moving randomly in the surrounding environment, acting as reflectors or absorbers, on the received power and delay spread are urgently needed. To enable these, new measurements campaigns are required based on channel sounders designed specifically to capture the realtime dynamics of the channel responses. This paper proposes a new methodology to enable fully dynamic measurements with a pseudonoise (PN)-sequence channel sounder by means of quasi-perfect transmitter-receiver (Tx-Rx) synchronization and suppression of probing signal effects in the post-processed channel impulse responses (CIRs). This approach allows the identification of the weak multipath components (MPCs) originated by reflections on the human body. The approach is validated by analysing CIRs collected in an indoor environment with one person moving close to the 60 GHz link. The results also demonstrate that future mmWave systems could exploit these additional MPCs and benefit from human interactions.

### 1 Introduction

Fifth generation (5G) wireless communications systems rely on mmWave spectrum [1] to enable very high data rates and low-latency services, due to the availability of very large bandwidths. High time resolution makes mmWaves signals suitable for accurate sensing, opening interesting perspectives for the emerging integrated sensing and communications (ISAC) techniques. At 60 GHz, regulations worldwide made available about 7 GHz of bandwidth for unlicensed operation; while the next release of the 5G New Radio (NR) standard will expand its frequency range to 71 GHz.

The peculiarities of the wireless medium at mmWaves prevent the simple extension of existing channel models for lower bands and require using appropriate sounding equipment for new measurements. A variety of channel sounders

have been developed for measurements in both outdoor (street canyon, rural, etc.) and indoor (home, office, etc.) scenarios [2]. Recently, the IEEE launched a dedicated Standardization Group (i.e. the IEEE SA - P2982 [3]) to recommend methods for verifying mmWave channel sounder performance based upon comparison of processed channel measurement data to either theory or an artifact having known characteristics.

Sounding can be carried out using different techniques that depend on the probe signal and processing methodology, i.e. multitone sounding [4], chirp sounders [5], PN-sequence sounders [6, 7], sliding correlator sounders [8], or VNA measurement setup [9]. These channel sounders, except the VNA-based, are all real-time capable and can thus measure dynamic effects; sounders that combine these signaling forms with switched (phased) arrays, e.g., [4, 10], enable even directionally resolved real-time measurements. For the considered large bandwidths, accurate synchronization is a major challenge. In [11] the importance of having an absolute timing reference to identify exactly the MPCs and their time of arrival for a thorough characterization of the dynamic propagation channel is highlighted and an effective channel sounding setup is proposed.

Measuring and modeling the impact of human bodies is essential as they can play a significant role as blockers or scatterers, especially in indoor environments. For this reason, several papers have investigated the blockage of a LOS connection by a human body, e.g., [12, 13, 14, 15, 16, 17, 10, 18, 19] who measured the attenuation of the LOS component as a function of the position of the intervening human body. An study of the shadowing loss of the human body at multiple mmWave bands has been presented in [16], relying on real-time channel measurements in an open office environment set-up by the channel sounder in [20]. Dynamic measurements of human interactions at mmWaves have been also performed in [17] at 28 GHz. At 60 GHz several other contributions developed measurement-based models for human blockage [18, 10, 19]. Recently, we provided in [21] a statistical analysis of the interaction of multipath and human bodies in a 60 GHz channel in an indoor environment for the cases of one and two human bodies.

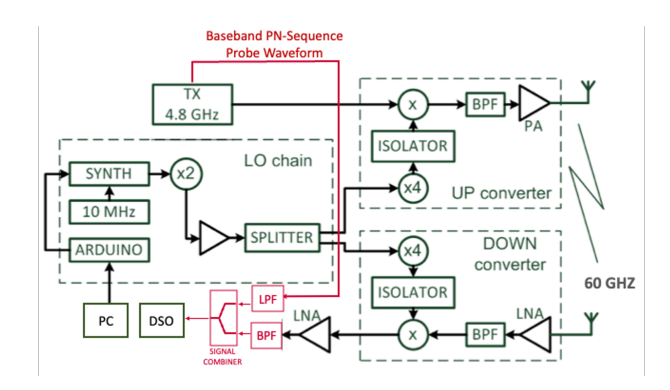


Figure 1. Experimental setup.

We derived a statistical model of the induced multipath effect, and discussed the impact of human presence on the statistical properties of channels. However, also this study is based on the static "evolutionary" measurements scenarios presented in [22]. To determine the multipath created by moving human bodies, a precise knowledge of the transmitted waveform and accurate timing is required, so that the (weak) human-reflected signals can be distinguished from, possibly time-varying, deviations of the transmitted signal from the nominal waveform caused by synchronization errors.

In this paper, we present a methodology for PN-sequence channel sounders to achieve quasi-perfect synchronization between the transmitted and received waveforms and a post-processing procedure to remove all artifacts introduced by the equipment on recorded CIRs, including the probing PN-sequence. This allows a complete and realistic characterization of the wireless channel in the presence of moving human bodies with reliable identification of MPCs originated by reflections on the body. We validate this approach showing the CIRs measured in the presence of a human body moving in the proximity of the radio link and standing behind the Rx. The originated MPCs are clearly visible in the multipath profiles and can be characterized.

### 2 MmWave Dynamic Channel Sounder

The block diagram of the channel sounder is shown in Fig. 1, where the red drawing shows the setup updates w.r.t. [6, 22] implementing the new methodology that enhances the channel sounder capability to record dynamic wireless CIRs. The Tx generates a baseband (BB) PN-sequence, with a bandwidth  $B^{BB} = 600$  MHz, that is up-converted to an Intermediate Frequency (IF) signal (4.2-5.4 GHz) [6]. Both signals are available as outputs of the Tx platform. The IF signal is then up-converted to the 60 GHz band, sent through a power amplifier (PA) and transmitted from a vertically polarized horn antenna with gain 15 dBi and beamwidth 30 degrees, mounted on a platform. The Rx antenna is omni-directional with a nominal gain of 2 dBi and vertical polarization. The local oscillator (LO) chain, feeding both the up- and down-converters, is equipped with a tunable synthesizer, whose output is multiplied by a factor

of 8, thus allowing the carrier frequency to be programmed at will in the frequency range from 54 to 66 GHz. Passband filters are also added in the up- and down-converters for the 54-59 GHz and 61-66 GHz bands. The architecture of the down-converter is complementary to the up-converter. The down-converter output signal at the IF  $f_c^{IF} = 4.78$  GHz is amplified and sent to a digital sampling oscilloscope (DSO) that can acquire signals up to 6 GHz with a 20 GSps sampling frequency. The tuning of the synthesizer and the waveform acquisition by the DSO are software controlled. We refer the reader to [6] and [22] for further details. The adds-on to the measurement setup described above consist of the combiner placed at the output of the down-converter that takes as inputs both the probe signal at the 4.78 GHz IF and the BB PN sequence probe generated at the Tx. This is exactly the same sequence used to get the IF probing waveform. Before entering into the combiner, these two signals are filtered by analog filters, to avoid undesired interference. The combiner's output is then injected into the DSO.

# 2.1 Post-processing procedure for quasiperfect synchronization

The DSO output signal is the combination of the BB PN sequence and the full received probing signal at 4.78 GHz down-converted from the 60 GHz band. We may easily isolate the BB and the IF signal by applying a digital lowpass filter and a pass-band filter, respectively. The IF signal is then demodulated to get the BB In-phase and Q-phase components and are then cross-correlated with the BB recovered signal in order to remove the probing waveform from the measured profiles. Since the received signal is the BB waveform, shifted to IF and 60 GHz frequency, passed through the wireless channel, the quasi-perfect synchronisation is inherent in the process.

The synchronization performance is evaluated by analysing the LOS components from all recorded profiles at a fixed distance and estimating the mismatch in the times of arrival. As shown in Fig. 2, the value of this mismatch is given by  $\Delta t = \pm 2 \cdot t_s$  where  $t_s$  is the applied sampling interval. Hence, it is related to DSO performance and can be reduced if a very short  $t_s$  is applied. For our DSO it ranges from -100 ps to 100 ps.

After the decorrelation, the CIRs are obtained by processing the recorded profiles with the CLEAN algorithm [23], a successive interference cancellation approach for deconvolution that estimates the arrival times and amplitudes of MPCs [22].

### 3 Validation Tests and Performance

The channel is sounded in a typical office environment with the antennas placed in fixed positions at a distance of 6 m and a height of 1.35 m. The carrier frequency of the probing signal is 57.5 GHz. Each acquisition record consists of

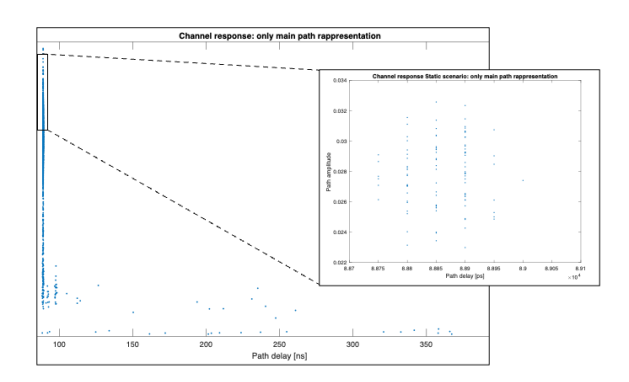
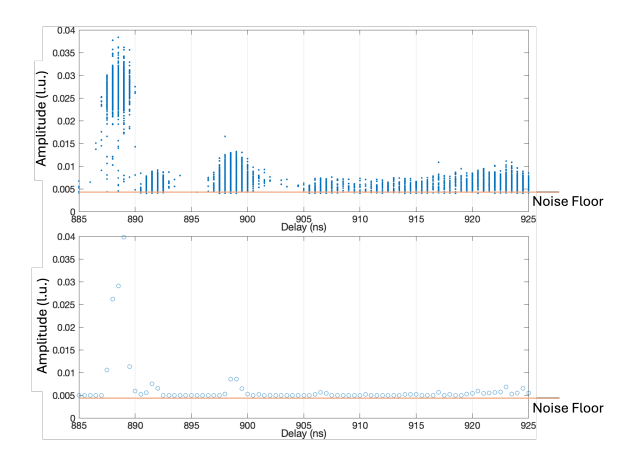


Figure 2. Synchronization evaluation.

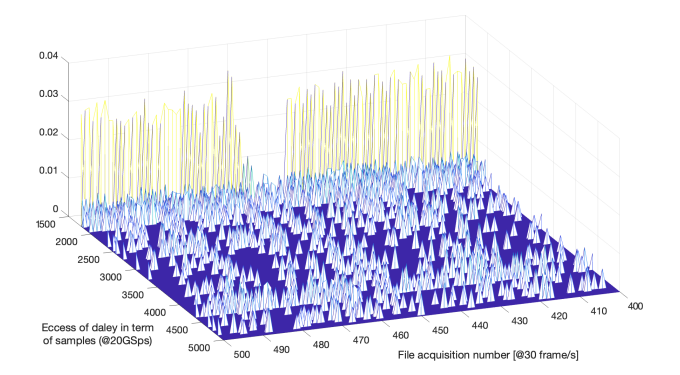
100 kSample at 30 frames per second. From each recorded file, a CIR sample is extracted. The scenario under test involves one person moving on a defined walking path between the Tx and Rx antennas, involving the following two phases: 1) crossing the LOS link; 2) standing behind the receiving antenna.

Fig. 4 shows the CIR samples vs. the excess delay, recorded continuously over an observation window of about 120 s, while the person is moving around. We can clearly observe the crossing point, associated with a deep fading episode of the CIRs around frame # 460. Close to the obstructed main path, we can spot additional MPCs that are related to the interactions with the human body. This is especially evident for the last phase "standing behind the receiver," where a strong MPC, not visible in the previous phases, appears at a delay close to the LOS path.

This phase is analysed in details in the upper plot of Fig. 3, in comparison with the static measurement with the empty room (lower plot). We can clearly spot the increase in the MPCs due to the human presence and the significant spreading at large delay, likely due to the scattering of the additional MPCs originated by the human body. This effect is evident in Fig, 5 where we distinguish three regions associated to the empty room ("Nobody"), the person "Walk-



**Figure 3.** Comparison between the profiles recorded with the dynamic human body moving around the receiver (up) and the static measurement with the empty room (down).



**Figure 4.** CIRs recorded during the crossing phase. LOS path blockage due to the crossing person at the frame # 460.

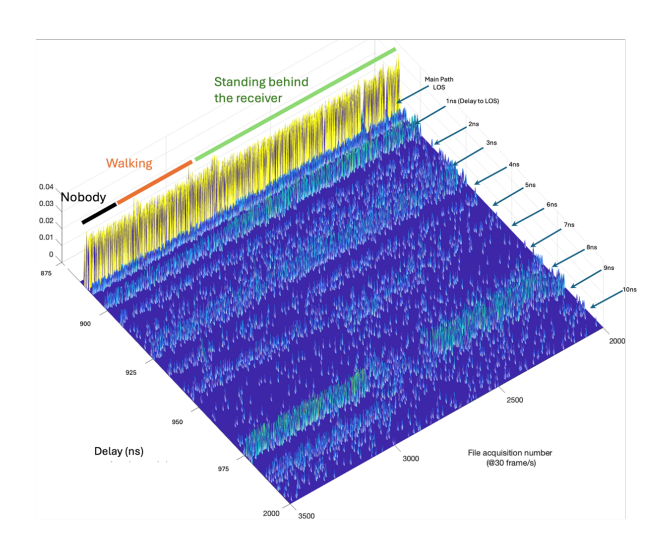


**Figure 5.** Dynamic CIRs with and without human interactions. Additional clutter at about 1, 3 and 6 ns is generated by interactions of human body and environment, whereas multipath blockage is visible at about 8.5 and 10 ns.

ing" and the person "Standing behind the receiver," as indicated by the upper bar over the CIRs plot. The standing position is not fixed but varies with time.

At a delay of about 1 ns from the LOS path additional MPCs appear, impacted by the interactions with the human body standing in the proximity of the Rx, and decay starting from the frame # 3000, when the person starts walking out from the coverage of the TX antenna. The same behaviour is observed at 3 and 6 ns (additional MPCs are generated from the frame # 2400).

At about 8.5 ns delay the human body produces a multipath blockage for a duration of 300 frames (about 10 s) in the frames # 2600–2900. The MPC at 10 ns appears only when the human body moves away from the Rx, i.e. it is a MPC generated by the environment, but obscured by the human body standing behind the Rx, i.e., at the frame # 3000.

### 4 Conclusion

In this paper we presented a methodology to achieve quasi-perfect synchronization between a mmWave channel sounder Tx and Rx such that accurate modeling of dynamic wireless channels is possible. We focused on the analysis of human interactions with mmWave MPCs. We have shown that an accurate characterization of the dynamic CIRs can be done with a low-cost PN channel sounder by relying on a quasi-perfect Tx-Rx synchronization and an accurate decorrelation of the recorded PN sequences with the synchronized template extracted instantaneously from the channel sounder. The MPCs of the post-processed CIRs can be easily correlated with the positions of the human bodies wrt the LOS link. The analysis of sample measurements demonstrates that the human interactions can be beneficial for the 60 GHz link, producing additional MPCs that contribute to the overall SNR at the Rx.

**Acknowledgment** This work was partially supported by the Italian Government under the programme PRIN-PNRR-2022 UPWARDS CUP E53D23014490001. The work of AFM was supported by the National Science Foundation.

### References

- [1] M. Shafi, A. F. Molisch, P. J. Smith, T. Haustein, P. Zhu, P. De Silva, F. Tufvesson, A. Benjebbour, and G. Wunder, "5G: A tutorial overview of standards, trials, challenges, deployment, and practice," *IEEE JSAC*, vol. 35, no. 6, 2017.
- [2] T. S. Rappaport, K. A. Remley, C. Gentile, A. F. Molisch, and A. Zajić, Radio Propagation Measurements and Channel Modeling: Best Practices for Millimeter-Wave and Sub-Terahertz Frequencies. Cambridge University Press, 2022.
- [3] IEEE SA P2982, (Accessed on 12/11/2023). [Online]. Available: https://standards.ieee.org/ieee/2982/10545/
- [4] C. U. Bas, R. Wang, S. Sangodoyin, D. Psychoudakis, T. Henige, R. Monroe, J. Park, C. J. Zhang, and A. F. Molisch, "Real-time millimeter-wave MIMO channel sounder for dynamic directional measurements," *IEEE Transactions on Vehicular Technology*, vol. 68, no. 9, pp. 8775–8789, 2019.
- [5] J. Osa, I. Barrutia, J. Cifuentes, I. Val, and M. Mendicute, "A Cost-Effective Directional Millimeter-Wave Channel Sounder for 60 GHz Industrial Wireless Communications," in 2022 IEEE 18th International Conference on Factory Communication Systems (WFCS), 2022.
- [6] S. Piersanti, L. A. Annoni, and D. Cassioli, "Millimeter waves channel measurements and path loss models," in 2012 IEEE International Conference on Communications (ICC), 2012, pp. 4552–4556.
- [7] T. Zwick, T. Beukema, and H. Nam, "Wideband channel sounder with measurements and model for the 60 GHz indoor radio channel," *IEEE Transactions on Vehicular Tech*nology, vol. 54, no. 4, 2005.
- [8] G. R. MacCartney and T. S. Rappaport, "A flexible millimeter-wave channel sounder with absolute timing," *IEEE Journal on Selected Areas in Communications*, vol. 35, no. 6, pp. 1402–1418, 2017.

- [9] X. Wu, C.-X. Wang, J. Sun, J. Huang, R. Feng, Y. Yang, and X. Ge, "60-ghz millimeter-wave channel measurements and modeling for indoor office environments," *IEEE Transactions on Antennas and Propagation*, vol. 65, no. 4, pp. 1912–1924, 2017.
- [10] C. Slezak, A. Dhananjay, and S. Rangan, "60 GHz blockage study using phased arrays," in *IEEE Asilomar Conf. on Signals, Systems, and Computers*, 2017.
- [11] D. Bodet, P. Dinh, M. Stojanovic, J. Widmer, D. Koutsonikolas, and J. M. Jornet, "Characterizing sub-thz mimo channels in practice: a novel channel sounder with absolute time reference," in *IEEE GLOBECOM 2023*.
- [12] C. Gustafson and F. Tufvesson, "Characterization of 60 ghz shadowing by human bodies and simple phantoms," in 2012 6th European Conference on Antennas and Propagation (EUCAP), 2012, pp. 473–477.
- [13] B. Peng, S. Rey, D. M. Rose, S. Hahn, and T. Kuerner, "Statistical Characteristics Study of Human Blockage Effect in Future Indoor Millimeter and Sub-Millimeter Wave Wireless Communications," in 2018 IEEE Vehicular Technol. Conf. (VTC Spring), 2018.
- [14] L. Ahumada Fierro, E. C. Maggi, A. Anglès Vazquez, and D. Schkolnik, "Empirical results for human-induced shadowing events for indoor 60 GHz wireless links," *IEEE Ac*cess, vol. 8, pp. 44 522–44 533, 2020.
- [15] M. Jacob, S. Priebe, R. Dickhoff, T. Kleine-Ostmann, T. Schrader, and T. Kurner, "Diffraction in mm and submm wave indoor propagation channels," *IEEE Trans. on Mi*crowave Theory and Techniques, 2012.
- [16] A. Al-Jzari, J. Huang, and S. Salous, "Mmwave indoor human blockage measurements and modeling at 26, 62, and 70 ghz bands," in 2023 XXXVth General Assembly and Scientific Symposium of the International Union of Radio Science (URSI GASS), 2023.
- [17] T. Choi, C. U. Bas, R. Wang, S. Hur, J. Park, J. Zhang, and A. F. Molisch, "Measurement Based Directional Modeling of Dynamic Human Body Shadowing at 28 GHz," in 2018 IEEE Global Communications Conference (GLOBECOM), 2018.
- [18] U. T. Virk and K. Haneda, "Modeling human blockage at 5G millimeter-wave frequencies," *IEEE Transact. on Antennas and Propagation*, vol. 68, no. 3, 2019.
- [19] A. Bhardwaj, D. Caudill, C. Gentile, J. Chuang, J. Senic, and D. G. Michelson, "Geometrical-empirical channel propagation model for human presence at 60 GHz," *IEEE Access*, vol. 9, 2021.
- [20] S. Salous, S. M. Feeney, X. Raimundo, and A. A. Cheema, "Wideband MIMO Channel Sounder for Radio Measurements in the 60 GHz Band," *IEEE Transactions on Wireless Communications*, vol. 15, no. 4, 2016.
- [21] B. A. A. Modad, D. Cassioli, and A. F. Molisch, "Analysis of the Multipath Effect of Human Presence on Indoor 60 GHz Wireless Channels," in *ICC* 2023 *IEEE International Conference on Communications*, 2023.
- [22] D. Cassioli and N. Rendevski, "A statistical model for the shadowing induced by human bodies in the proximity of a mmWaves radio link," in *IEEE Internat. Conf. on Communicat. Workshops*, 2014.
- [23] J. A. Högbom, "Aperture Synthesis with a Non-Regular Distribution of Interferometer Baselines," *Astronomy and Astrophysics Suppl.*, vol. 15, Jun. 1974.